Diabetologia (2022) 65:1032–1047
https://doi.org/10.1007/s00125-022-05676-8

ARTICLE

Loss of function of renal *Glut2* reverses hyperglycaemia and normalises body weight in mouse models of diabetes and obesity

Leticia Maria de Souza Cordeiro[1] · Lauren Bainbridge[1] · Nagavardhini Devisetty[1] · David H. McDougal[2] · Dorien J. M. Peters[3] · Kavaljit H. Chhabra[1,4]

Received: 24 August 2021 / Accepted: 5 January 2022 / Published online: 15 March 2022

Abstract

Aims/hypothesis Renal GLUT2 is increased in diabetes, thereby enhancing glucose reabsorption and worsening hyperglycaemia. Here, we determined whether loss of *Glut2* (also known as *Slc2a2*) specifically in the kidneys would reverse hyperglycaemia and normalise body weight in mouse models of diabetes and obesity.

Methods We used the tamoxifen-inducible CreERT2-Lox system in mice to knockout *Glut2* specifically in the kidneys (Ks-*Glut2* KO) to establish the contribution of renal GLUT2 to systemic glucose homeostasis in health and in insulin-dependent as well as non-insulin-dependent diabetes. We measured circulating glucose and insulin levels in response to OGTT or IVGTT under different experimental conditions in the Ks-*Glut2* KO and their control mice. Moreover, we quantified urine glucose levels to explain the phenotype of the mice independently of insulin actions. We also used a transcription factor array to identify mechanisms underlying the crosstalk between renal GLUT2 and sodium–glucose cotransporter 2 (SGLT2).

Results The Ks-*Glut2* KO mice exhibited improved glucose tolerance and massive glucosuria. Interestingly, this improvement in blood glucose control was eliminated when we knocked out *Glut2* in the liver in addition to the kidneys, suggesting that the improvement is attributable to the lack of renal *GLUT2*. Remarkably, induction of renal *Glut2* deficiency reversed hyperglycaemia and normalised body weight in mouse models of diabetes and obesity. Longitudinal monitoring of renal glucose transporters revealed that *Sglt2* (also known as *Slc5a2*) expression was almost abolished 3 weeks after inducing renal *Glut2* deficiency. To identify a molecular basis for this crosstalk, we screened for renal transcription factors that were downregulated in the Ks-*Glut2* KO mice. *Hnf1α* (also known as *Hnf1a*) was among the genes most downregulated and its recovery restored *Sglt2* expression in primary renal proximal tubular cells isolated from the Ks-*Glut2* KO mice.

Conclusions/interpretation Altogether, these results demonstrate a novel crosstalk between renal *GLUT2* and *SGLT2* in regulating systemic glucose homeostasis via glucose reabsorption. Our findings also indicate that inhibiting renal GLUT2 is a potential therapy for diabetes and obesity.

Keywords Diabetes · Glucose homeostasis · Glucose transporters · GLUT2 · Mouse models · Obesity · SGLT2

Leticia Maria de Souza Cordeiro and Lauren Bainbridge contributed equally to this study.

✉ Kavaljit H. Chhabra
Kavaljit_Chhabra@URMC.Rochester.Edu

[1] Department of Medicine, Division of Endocrinology, Diabetes and Metabolism, University of Rochester School of Medicine and Dentistry, Rochester, NY, USA

[2] Pennington Biomedical Research Center, Louisiana State University, Baton Rouge, LA, USA

[3] Department of Human Genetics, Leiden University Medical Center, Leiden, the Netherlands

[4] Department of Pharmacology and Physiology, University of Rochester Medical Center, Rochester, NY, USA

Research in context

What is already known about this subject?

- GLUT2 is a major glucose transporter in the kidneys
- Diabetes increases renal GLUT2 levels, which in turn enhances glucose reabsorption and worsens already elevated blood glucose levels

What is the key question?

- Would loss of function of renal *Glut2* (also known as *Slc2a2*) alone reverse hyperglycaemia and reduce body weight in mouse models of diabetes and obesity?

What are the new findings?

- Genetic loss of renal *Glut2* normalises blood glucose levels and body weight in mouse models of diabetes and obesity
- Long-term renal *Glut2* deficiency abolishes the expression of renal *Sglt2* via the transcription factor HNF1α

How might this impact on clinical practice in the foreseeable future?

- Blocking renal GLUT2 can potentially treat diabetes and obesity, a strategy that may overcome some of the limitations of current SGLT2 inhibitors

Abbreviations

GSIS	Glucose-stimulated insulin secretion
HFSD	High-fat + sucrose diet
HNF1α	Hepatocyte nuclear factor-1α
KO	Knockout
Ks-*Glut2* KO	*Glut2* knocked out specifically in the kidneys
SGLT1	Sodium–glucose cotransporter 1
SGLT2	Sodium–glucose cotransporter 2
STZ	Streptozotocin
TBST	Tris-buffered saline with 0.1% Tween 20 detergent

Introduction

GLUT2 is a major facilitative glucose transporter expressed in the basolateral membrane of the epithelial cells predominantly in the liver, kidneys and intestine [1, 2]. It is also present in rodent beta cells [3, 4]; however, some reports suggest that GLUT2 is not a major glucose transporter in human beta cells [4, 5]. *GLUT2* (also known as *SLC2A2*) mutations cause Fanconi–Bickel syndrome [6, 7], which is characterised by glucose malabsorption, glycogen accumulation and renal glucosuria. Although this syndrome does not cause fasting hyperglycaemia [6, 7], it may lead to transient neonatal diabetes [8, 9]. This phenotype is in contrast to that observed in global *Glut2* knockout (KO) mice, which exhibit overt diabetes [3, 10]. Renal GLUT2 facilitates most of the glucose reabsorption in concert with sodium–glucose cotransporter 2 (SGLT2), which is located at the apical membrane of renal proximal tubular cells and is an established target in the treatment of diabetes [11–18]. Diabetes increases renal GLUT2 levels in humans and rodents [19–25], which further worsens hyperglycaemia because of enhanced glucose reabsorption. Therefore, blocking renal GLUT2 may ameliorate hyperglycaemia by interfering with this vicious cycle. Yet, it is unknown whether loss of function of renal *GLUT2* would adequately elevate glucosuria to reverse hyperglycaemia to the degree that is accomplished by SGLT2 inhibition [13–18]. Moreover, the physiological contribution of renal GLUT2 to systemic glucose homeostasis is not completely established.

Previous studies, including those from our laboratory, suggest that reducing renal GLUT2 may mitigate hyperglycaemia [24, 26–28]. For example, we recently reported that reduction of GLUT2 levels in the kidneys improves glucose tolerance in hypothalamus-specific pro-opiomelanocortin (POMC) or melanocortin 4 receptor (MC4R) KO mice despite obesity and insulin resistance [27, 28]. Nevertheless, whether lack of renal GLUT2 would reverse hyperglycaemia in mouse models of diabetes and obesity remains unknown. To answer this question, we generated mice in which renal *Glut2* can be knocked out at a desired time using the tamoxifen-inducible CreERT2-Lox system. Moreover, we produced and characterised a mouse model that lacks *Glut2* in the liver in addition to the kidneys to further validate the precise contribution of renal GLUT2 in regulating blood glucose relative to other major tissues expressing this glucose transporter. Besides establishing the physiological role of renal GLUT2 in systemic glucose homeostasis and its therapeutic potential in diabetes and obesity in this study, we investigated whether and how the loss of renal *Glut2* affects the gene expression of other renal glucose transporters.

Methods

Study design and mouse models All animal procedures were approved by the Institutional Animal Care and Use Committee at the University of Rochester, Pennington Biomedical Research Center, or the University of Alabama at Birmingham, and were performed according to the US Public Health Service guidelines for the humane care and use of experimental animals. Mice were housed in ventilated cages under controlled temperature (~23°C) and photoperiod (12 h light–dark cycle, lights on from 06:00 hours to 18:00 hours) conditions with free access to Hydropac water (Lab Products, USA) and regular laboratory chow (5010; LabDiet, USA). After genotyping, mice were randomly assigned to different experimental groups. We used two mouse lines with their littermate controls in this study: *KspCad*^{CreERT2};*Glut2*$^{loxP/loxP}$ mice with induced renal *Glut2* deficiency; and *Ggt1*^{Cre};*Glut2*$^{loxP/loxP}$ mice with knockout of *Glut2* in the liver in addition to the kidneys.

We generated *Glut2*$^{loxP/loxP}$ (also known as *Slc2a2*$^{loxP/loxP}$) mice (received from D. McDougal, Pennington Biomedical Research Center, Baton Rouge, LA, USA) using heterozygous *Glut2*$^{tm1a(KOMP)Wtsi}$ mice that were produced using ES cells obtained from the Knockout Mouse Project at the University of California, Davis (project ID: CSD40514; MMRRC:065826-UCD). ES cells were microinjected into albino C57BL/6J mouse blastocysts and the resulting chimeras were mated with B6(Cg)-*Tyr*$^{c-2J}$/J (B6-albino mice, 000058; The Jackson Laboratory, USA) for germline-derived F1 mice. F1 mice were mated with C57BL/6NTac mice for colony expansion. These founder mice were crossed with B6.Cg-Tg(ACTFLPe)9205Dym/J mice (005703; The Jackson Laboratory), which express the flippase recombinase to remove the lacZ and neomycin cassettes generating *Glut2*$^{loxP/loxP}$ mice (i.e. tm1a > tm1c allele conversion), which can be used for Cre-mediated *Glut2* inactivation (ESM Fig. 1a). To generate *KspCad*^{CreERT2};*Glut2*$^{loxP/loxP}$ and their littermate control mice, we first crossed the *Glut2*$^{loxP/loxP}$ mice with the *KspCad*^{CreERT2} mouse line [29, 30] (received from D. J. M. Peters, Leiden University Medical Center, Leiden, the Netherlands), followed by a second generation of intercrossing between *KspCad*^{CreERT2};*Glut2*$^{loxP/+}$ and *Glut2*$^{loxP/loxP}$ mice. The *KspCad*^{CreERT2} mice are validated to exhibit Cre expression in proximal tubules [29–31], wherein *Glut2* is also expressed predominantly. We used the same breeding strategy to produce *Ggt1*^{Cre};*Glut2*$^{loxP/loxP}$ mice from the *Ggt1*^{Cre} mouse line (012841; The Jackson Laboratory) resulting in *Glut2* knockout in the liver in addition to the kidneys. All the experimental mice used in this study were age-matched relative to their corresponding control groups.

We injected tamoxifen (50 mg/kg dissolved first in one part 100% ethanol by incubating the mixture at 60°C for 20 min, followed by addition of nine parts of sesame oil, T5648 and S3547 [Sigma, USA]) once daily for three consecutive days in *KspCad*^{CreERT2};*Glut2*$^{loxP/loxP}$ mice to induce *Glut2* deficiency in the kidneys. All of the experiments, except those using a diet-induced obesity mouse model or noted otherwise, were completed within 14 days of inducing the *Glut2* deficiency. To produce the mouse model of type 1 diabetes, we administered freshly prepared streptozotocin (STZ; 80 mg/kg dissolved in citric acid–sodium citrate buffer, pH 4.5, i.p.; S0130; Sigma) once daily for five consecutive days. The mice exhibited hyperglycaemia (>14 mmol/l glucose) by 24 days after the first STZ injection. To induce obesity and insulin resistance in mice used in this study, immediately after weaning we fed them with high-fat + sucrose diet (HFSD; D12331; Research Diets, USA), or the regular laboratory chow to the control group, for 20 weeks and measured their metabolic variables. After the baseline measurements, we induced renal *Glut2* deficiency and the mice continued to receive their corresponding diets for an additional 5 weeks. We measured body weight and food intake of these mice once a week for the duration of the study. Experimenters were not blinded to group assignment and outcome assessment. We did not exclude any data, samples or mice in reporting the results of this study.

Reverse transcription quantitative PCR An E.Z.N.A kit (101319-260; Omega, USA) was used to extract total RNA from the renal cortex, liver or primary renal proximal tubular cells. We used 500 ng total RNA and random hexamer primers (1708891; iScript cDNA synthesis kit; BioRad, USA) to generate cDNA. Reverse transcription quantitative PCR (RT-qPCR) was performed using a StepOne Real Time PCR System (Applied Biosystems, USA) and SYBR green master mix (1725124; BioRad). We used the following primers: for *Glut2* (*Slc2a2*), 5′-GAA GGA ACT CAG TAC AGC AGT G-3′ and 5′-TCA TCC ACA TTC AGT ACA GGA C-3′; for *Sglt2* (*Slc5a2*), 5′-AGT GTC TGT GTA CAT CAG TGC-3′ and 5′-CAA GAT CTC GGT GGA TAT GTT CTC-3′; for *Glut1* (*Slc2a1*), 5′-GTG GTG AGT GTG GAT G-3′ and 5′-AGT TCG GCT ATA ACA CTG GTG-3′; for *Sglt1* (*Slc5a1*), 5′-CAA TCA GCA CGA GGA TGA ACA-3′ and 5′-GCT CCT TGA CCT CCA TCT TC-3′; for *Hnf1α* (*Hnf1a*), 5′-AGA GAC CTT GGT GGA GTG T-3′ and 5′-GGC AAA CCA GTT GTA GAC ACG C-3′; for *G6pc*, 5′-AGG TCG TGG CTG GAG TCT TGT C-3′ and 5′-GTA GCA GGT AGA ATC CAA GCG C-3′; for *Pck1α*, 5′-GGC GAT GAC ATT GCC TGG ATG A-3′ and 5′-TGT CTT CAC TGA GGT GCC AGG A-3′; and for *Hprt*, 5′-AAC AAA GTC TGG CCT GTA TCC-3′ and 5′-CCC CAA AAT GGT TAA GGT TGC-3′. All primers were used at a final concentration of 500 nmol/l. The relative quantity of each mRNA was calculated from standard curves and normalised to the internal control *Hprt*, and then normalised to the mean of corresponding controls.

Immunohistochemistry, western blotting, and proteomics We embedded formalin (10% neutral buffered)-fixed kidneys in paraffin and cut 5 μm sections with a microtome. We mounted these sections onto slides for immunohistochemistry. We had deparaffinised and rehydrated the sections before incubating them in sodium citrate buffer (pH 6.0) at 95°C in a water bath for 20 min for antigen retrieval. After the antigen retrieval step, we rinsed the slides three times (10 min/wash) in tris-buffered saline with 0.1% Tween 20 detergent (TBST) buffer and blocked the sections in 10% normal goat serum for 2 h. We then incubated the sections overnight at 4°C with the following primary antibodies: rabbit anti-GLUT2 (600-401-GN3 [Rockland Immunochemicals, USA] or ab54460 [Abcam, USA]; 1:500 dilution in TBST); mouse anti-SGLT2 (sc-393350; Santa Cruz Biotechnology, USA; 1:100 dilution in TBST); or mouse anti-HNF1α (sc-393925; Santa Cruz Biotechnology; 1:100 dilution in TBST). Following the incubation period, the sections were washed three times (10 min/wash) in TBST and then incubated with either secondary goat-anti-rabbit antibody conjugated to Alexa Fluor 594 (ab150080; Abcam; 1:1000 dilution in TBST) or goat-anti-mouse antibody conjugated to Alex Fluro 647 (ab150115; Abcam; 1:1000 dilution in TBST) for 1 h at room temperature. The sections were washed again three times (10 min/wash) in TBST and incubated for 1 h with lotus tetragonolobus lectin (FL-1321-2; Vector Laboratories, USA; 1:200 dilution in TBST) to label renal proximal tubules. After this incubation, the sections were washed with TBST (10 min, one wash) and counterstained with DAPI (D9542; Sigma; 1 μg/ml) for 1 min. The sections were washed again with TBST, then the slides were air-dried and coverslipped using ProLong Antifade mounting medium (P36930; Molecular Probes, USA). Images were captured using Keyence fluorescence microscope BZ-X800. We quantified the images using the NIH ImageJ software, version 1.53n (https://imagej.nih.gov/ij/download.html).

We performed western blotting to measure renal GLUT2 and hepatocyte nuclear factor-1α (HNF1α) as described previously [27, 28, 32] using these primary and secondary antibodies: anti-GLUT2 (600-401-GN3; Rockland Immunochemicals, USA; 1:2000 dilution in TBST), anti-HNF1α (89670; Cell Signaling Technology, USA; 1:2000 dilution in TBST) and anti-rabbit secondary antibody (NA934; GE Healthcare, USA; 1:5000 dilution in TBST). We had either cut the blots horizontally just above ~80 KDa to examine the internal control at the same time as the proteins of interest on the same membrane or we had stripped the blots to remove antibodies after imaging proteins of interest and used the same blots for probing the internal control. We used ECL substrate (34095; Thermo Fisher Scientific, USA) to produce luminescence that was recorded on a BioRad imaging system.

We used proteomics assay to validate the results obtained from the antibodies mentioned above and to further confirm the deficiency of renal GLUT2 protein in our new mouse model. Renal cortical trypsin-digested peptides, obtained from control and experimental mice, were injected onto a home-made 30 cm C18 column with 1.8 μm beads (Sepax, USA), with an Easy nLC-1200 HPLC (Thermo Fisher Scientific), connected to a Fusion Lumos Tribrid mass spectrometer (Thermo Fisher Scientific). Raw data was searched using the SEQUEST search engine within the Proteome Discoverer software platform, version 2.4 (Thermo Fisher Scientific), using the SwissProt *mus musculus* database. The Minora node was used to determine relative protein abundance between the samples using the Summed Abundance default settings. Percolator was used as the false discovery rate (FDR) calculator, filtering out peptides which had a q value greater than 0.01.

Primary mouse renal proximal tubular epithelial cells We isolated primary proximal tubular epithelial cells from mice with *Glut2* knocked out specifically in the kidneys (Ks-*Glut2* KO mice) and their littermate controls using a published protocol [33]. We cultured the cells in collagen-coated six-well plates (10^6 cells/well; A1142801; Thermo Fisher Scientific, USA) in renal epithelial cell basal medium (PCS-400-030; ATCC, USA) supplemented with the renal epithelial cell growth kit (PCS-400-040; ATCC). Two days after initiating the culture of these cells, we used them for either gene expression measurements or glucose transport assay.

For gene expression studies, we transfected the cells with *Hnf1α*-expressing plasmid (MC202766; OriGene Technologies, USA), control plasmid (PCMV6KN; OriGene Technologies) or *Glut2*-expressing plasmid (MG208388; OriGene Technologies) using TurboFectin transfection reagent (TF81001; OriGene Technologies) according to the manufacturer's protocol. Three days after the transfection, we extracted the RNA and used RT-qPCR to measure the mRNA levels of *Glut2*, *Sglt2* and *Hnf1α*.

Glucose transport assay We measured renal GLUT2 activity using a glucose transport assay. For this assay, we cultured the primary mouse renal proximal tubular epithelial cells in hanging inserts (MCRP24H48; Millipore, USA) as previously described [28]. We incubated the cells with Hank's balanced salt solution containing [$^{13}C_6$]glucose (5 mmol/l) in the presence or absence of the GLUT2 inhibitor phloretin (1 mmol/l in 1:1 DMSO/PBS; 14452; Cayman Chemical, USA). We then measured the labelled glucose at the basolateral (bottom) side of the cells at different times. The University of Rochester Mass Spectrometry Resource Laboratory measured $^{13}C_6$ glucose by LC-MS assay using a Shonex HILICpak VG-50 2D column.

OGTT, ITT and in vivo glucose-stimulated insulin secretion assay We performed OGTTs in mice fasted overnight (18:00–08:00 hours) or for 6 h (08:00–14:00 hours). For ITTs we fasted mice for 6 h (08:00–14:00 hours). On the day of the experiments we measured their baseline blood glucose levels (tail-vein blood; AlphaTRAK 2 glucometer; Zoetis, USA) at 0 min and administered glucose by oral gavage (100 mg/mouse in 300 μl 0.9% wt/vol. saline [154 mmol/l NaCl]; G8270; Sigma) or insulin by i.p. injection (15 mU/mouse; Humulin R; Eli Lilly, USA), followed by measurements of blood glucose levels at 15, 30, 60 and 120 min. In mice with STZ-induced diabetes, we administered only 15 mg glucose/mouse to assess glucose tolerance because a higher dose would have increased blood glucose levels beyond the sensitivity of the assay range due to this model's hyperglycaemia at baseline. To calculate the total AUC for the glucose measurements, we used the trapezoidal rule.

To assess glucose-stimulated insulin secretion (GSIS) in *KspCad*^{CreERT2};*Glut2*$^{loxP/loxP}$ mice and their littermate controls, we cannulated the carotid artery and jugular vein to administer glucose and collect blood in freely moving awake mice [27]. After the mice recovered from the surgery over a period of 3–5 days, on the day of the experiment, we fasted mice for 6 h (08:00–14:00 hours) and administered an i.v. bolus of 60 mg of glucose. After the glucose administration we measured blood glucose and insulin levels at different times. For GSIS assay in *Ggt1*^{Cre};*Glut2*$^{loxP/loxP}$ mice and their control littermates, we fasted mice for 6 h and collected tail blood using capillary tubes (22-362-566; Fisherbrand, USA) at baseline and at 20 min after oral challenge with 100 mg glucose.

For glucose tolerance studies involving the SGLT2 inhibitor dapagliflozin, we administered the drug by i.p. injection (5 mg/kg dissolved in 300 μl 0.9% wt/vol. saline; 11574; Cayman Chemical) 30 min prior to the GTTs.

Urine glucose, sodium and creatinine assays We placed mice individually in metabolic cages (Tecniplast, USA) and allowed them to acclimate to the cages for 3–5 days before collecting their 24 h urine under different experimental conditions. We used colorimetric assays to measure glucose (10009582; Cayman Chemical), sodium (MAK247; Sigma) and creatinine (500701; Cayman Chemical) levels in the urine according to the manufacturers' protocols.

For urine glucose studies involving dapagliflozin, we administered the drug by i.p. injection (5 mg/kg dissolved in 300 μl 0.9% wt/vol. saline) twice a day (09:00 and 17:00 hours) and collected urine 24 h after the first injection.

Plasma or serum measurements We collected the mouse trunk blood between 14:00 and 15:00 hours on the day of the experiments to obtain serum from mice in all the experimental groups. For plasma, we used heparinised capillary tubes (22-362-566; Fisherbrand) to draw tail-vein blood from the mice used in this study. We centrifuged the blood at 2000 *g* at 4°C for 20 min to separate plasma or serum from whole blood. We measured plasma insulin (90080; Crystal Chem, USA) and serum glucagon (81518; Crystal Chem) levels by ELISA. Serum creatinine (700460; Cayman Chemical), β-hydroxybutyrate (700190; Cayman Chemical) and NEFA (ab65341; Abcam) were measured by colorimetric assays. The absorbance was measured using a spectrophotometer as per the manufacturer's instructions (Epoch, BioTek, USA).

GFR, glomerular area and urine pH GFR in conscious mice was measured using a transdermal FITC–sinistrin clearance method [34] at the University of Alabama at Birmingham O'Brien Center. Mice were anaesthetised with isoflurane and FITC–sinistrin (MediBeacon, USA) solution injected via the tail vein. Data were analysed using MB Studio version 2.1 (MediBeacon). A three-compartment model with linear baseline correction term (CP3L) was used to provide best fit results, as relating to t½ measurements. The FITC–sinistrin t½ (in min) was converted to GFR (in μl/min) and normalised for individual mouse body weight.

For measuring the glomerular area, we used 5 μm kidney sections obtained from formalin-fixed paraffin embedded mouse kidneys. The sections were stained with H&E. Images of the sections were captured using an Olympus microscope with ×20 objective lens and analysed using the NIH ImageJ software version 1.53n, https://imagej.nih.gov/ij/download.html.

We measured urine pH using an electronic high resolution pH meter (HI2020-01; Hanna Instruments, USA).

PCR array For PCR array, the cDNA was mixed with nuclease-free water and SYBR Green master mix to prepare PCR components mix. We added 25 μl of the components mix to each well of the mouse transcription factors PCR array plate (PAMM-075ZC; Qiagen, USA) and performed RT-qPCR as described above. The relative gene expression was calculated using the $2^{-\Delta\Delta C_t}$ method as per the manufacturer's instructions. We used β-actin as an internal control for the quantification of target genes.

Statistical analyses All data are presented as mean ± SEM and were analysed by two-tailed Student's paired or unpaired *t* test, one-way ANOVA or two-way ANOVA followed by a Bonferroni post hoc multiple comparison test when appropriate. All analyses were performed using Prism version 8.0.1 (GraphPad, USA) and differences were considered statistically significant at $p<0.05$.

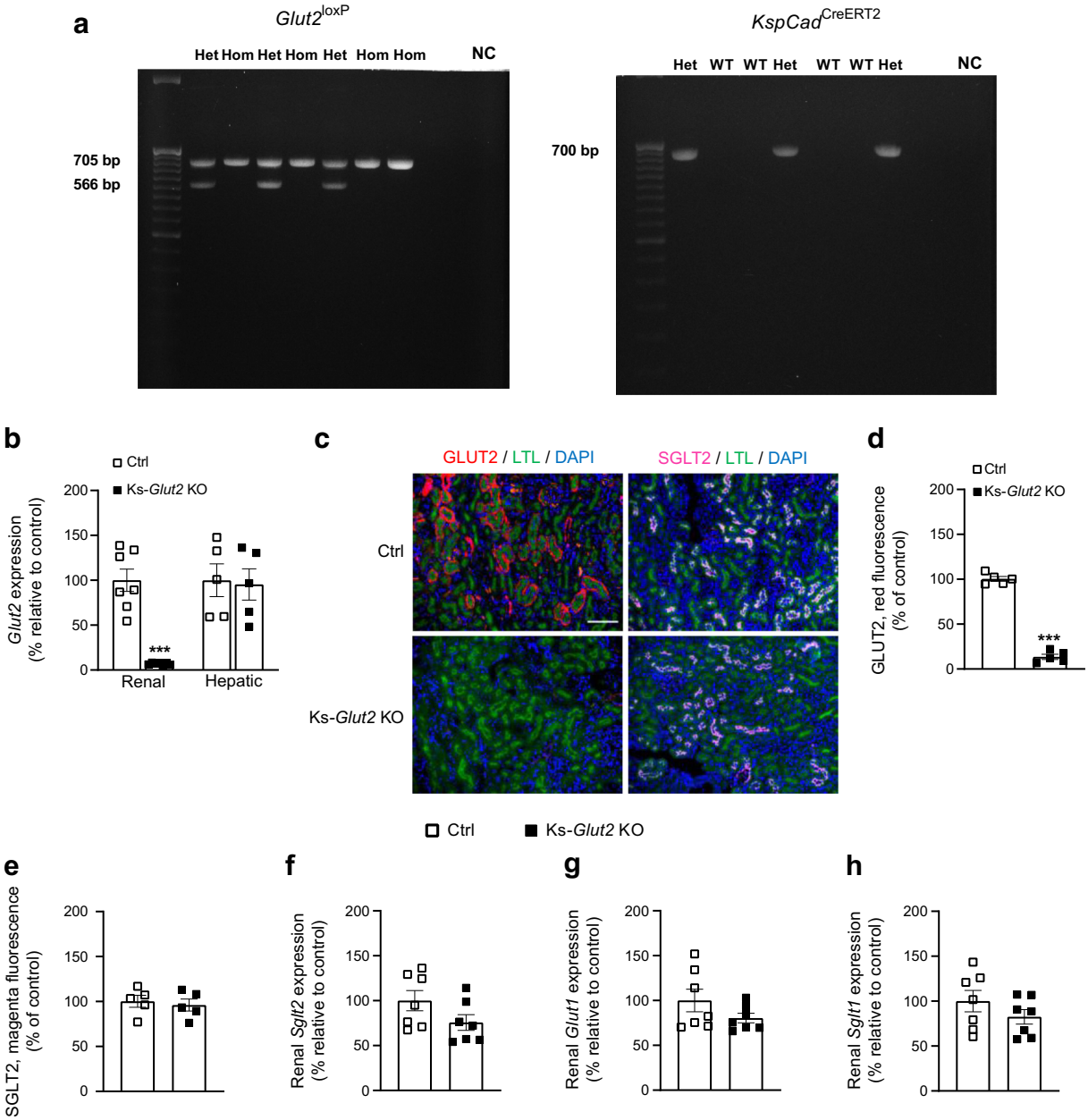

Fig. 1 Validation of inducible kidney-specific loss of *Glut2* in mice. (**a**) Representative genotypes of mice used in this study. *Glut2*^{loxP} mouse model: *Glut2*^{loxP} heterozygous (705 and 566 bp); *Glut2*^{loxP} homozygous (705 bp). *KspCad*^{CreERT2} mouse model: *KspCad*^{CreERT2} heterozygous (700 bp); WT (no band). (**b**–**e**) Expression of renal cortical and hepatic *Glut2* (**b**), and immunofluorescence staining of renal GLUT2 and SGLT2 (**c**), together with their quantification (**d**, **e**). Scale bar, 100 μm. (**f**–**h**) Expression of renal *Sglt2* (**f**), *Glut1* (**g**) and *Sglt1* (**h**). Data are shown as means ± SEM for 8- to 12-week-old male mice within 14 days of inducing renal *Glut2* deficiency, n = 5–7. ***p<0.001 vs Ctrl group (one-way ANOVA followed by Bonferroni's post hoc test or two-tailed unpaired Student's t test). Ctrl, control group; Het, heterozygous; Hom, homozygous; LTL, *Lotus tetragonolobus* lectin, a marker of renal proximal tubules; NC, negative control; WT, wild-type

Results

Generation and validation of mice showing inducible kidney-specific loss of *Glut2* We crossed the mouse line expressing tamoxifen-inducible Cre recombinase under the control of kidney-specific cadherin gene (*KspCad*^{CreERT2}) [29] with *Glut2*$^{loxP/loxP}$ mice (ESM Fig. 1a) to obtain *KspCad*^{CreERT2};*Glut2*$^{loxP/loxP}$ mice. The *KspCad*^{CreERT2} mouse line is well characterised for inducing gene modifications specific to the kidney, including proximal tubules where *Glut2* is predominantly present, using the Cre-Lox system [29–31]. We observed that the *KspCad*^{CreERT2};*Glut2*$^{loxP/loxP}$ mice exhibited deficiency of renal *Glut2* gene and GLUT2 protein as well as reduced glucose transport activity compared

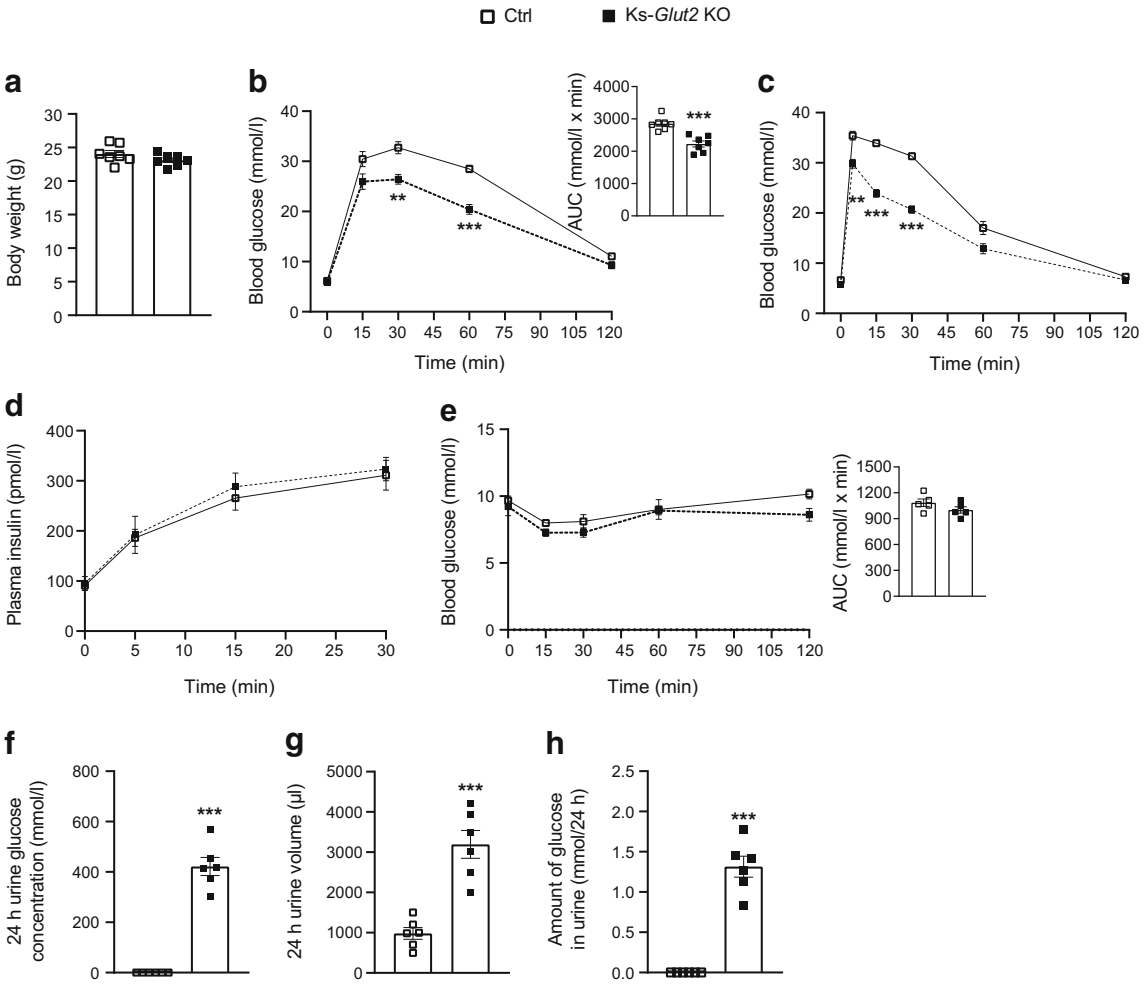

Fig. 2 Lack of renal *Glut2* improves glucose tolerance and elevates glucosuria in mice. (**a**) Body weight. (**b**) Blood glucose levels during OGTT, with corresponding AUC. (**c**) Blood glucose levels during IVGTT. (**d**) Plasma insulin levels during GSIS. (**e**) Blood glucose levels during ITT, with corresponding AUC. (**f**) 24 h urine glucose concentration. (**g**) 24 h urine volume. (**h**) 24 h amount of glucose in urine. Data are shown as means ± SEM for 8- to 12-week-old male mice within 14 days of inducing renal *Glut2* deficiency, $n = 5–7$. $^{**}p<0.01$ and $^{***}p<0.001$ vs Ctrl group (two-tailed unpaired Student's *t* test or repeated measures two-way ANOVA followed by Bonferroni's multiple comparison test). Ctrl, control group

with their littermate controls (*KspCad*^{CreERT2} or *Glut2*$^{loxP/loxP}$) following the administration of tamoxifen, without *Glut2* expression in the liver being affected (male mice, Fig. 1a–d and ESM Fig. 1b,c; female mice, ESM Fig. 2a). Moreover, the expression of other renal cortical glucose transporters in the experimental group was not different from that in the control group within 14 days of inducing the *Glut2* deficiency (male mice, Fig. 1c,e–h; female mice, ESM Fig. 2b–d). Overall, we have validated tamoxifen-inducible lack of *Glut2* specifically in the kidneys (Ks-*Glut2* KO) in the new mouse model.

Ks-*Glut2* KO mice exhibit improved glucose tolerance and intense glucosuria The Ks-*Glut2* KO mice had normal body weight, fasting blood glucose levels, and improved glucose tolerance (male mice, Fig. 2a–c; female mice, ESM Fig. 2e,f) without any changes in GSIS or insulin sensitivity (male mice, Fig. 2d,e; female mice, ESM Fig. 2g). The KO mice manifested polyuria and massive glucosuria (male mice, Fig. 2f–h; female mice, ESM Fig. 2h–j). Urine glucose concentration (Fig. 2f and ESM Fig. 2h) and urine volume (Fig. 2g and ESM Fig. 2i) were used to calculate the total amount of glucose excreted in 24 h (Fig. 2h and ESM Fig. 2j). Moreover, the Ks-*Glut2* KO mice exhibited polydipsia, natriuresis and reduced amount of urine creatinine compared with their littermate controls (ESM Fig. 3a–c) without any changes in food intake (control mice, 4.1 ± 0.3 g/day; Ks-*Glut2* KO mice, 3.9 ± 0.2 g/day). Together, these results demonstrate the physiological contribution of renal GLUT2 in regulating systemic glucose homeostasis by glucosuria.

The Ks-*Glut2* KO mice had normal serum glucagon, β-hydroxybutyrate, NEFA and creatinine levels (ESM Fig. 3d–g). Moreover, of the two major enzymes involved in hepatic

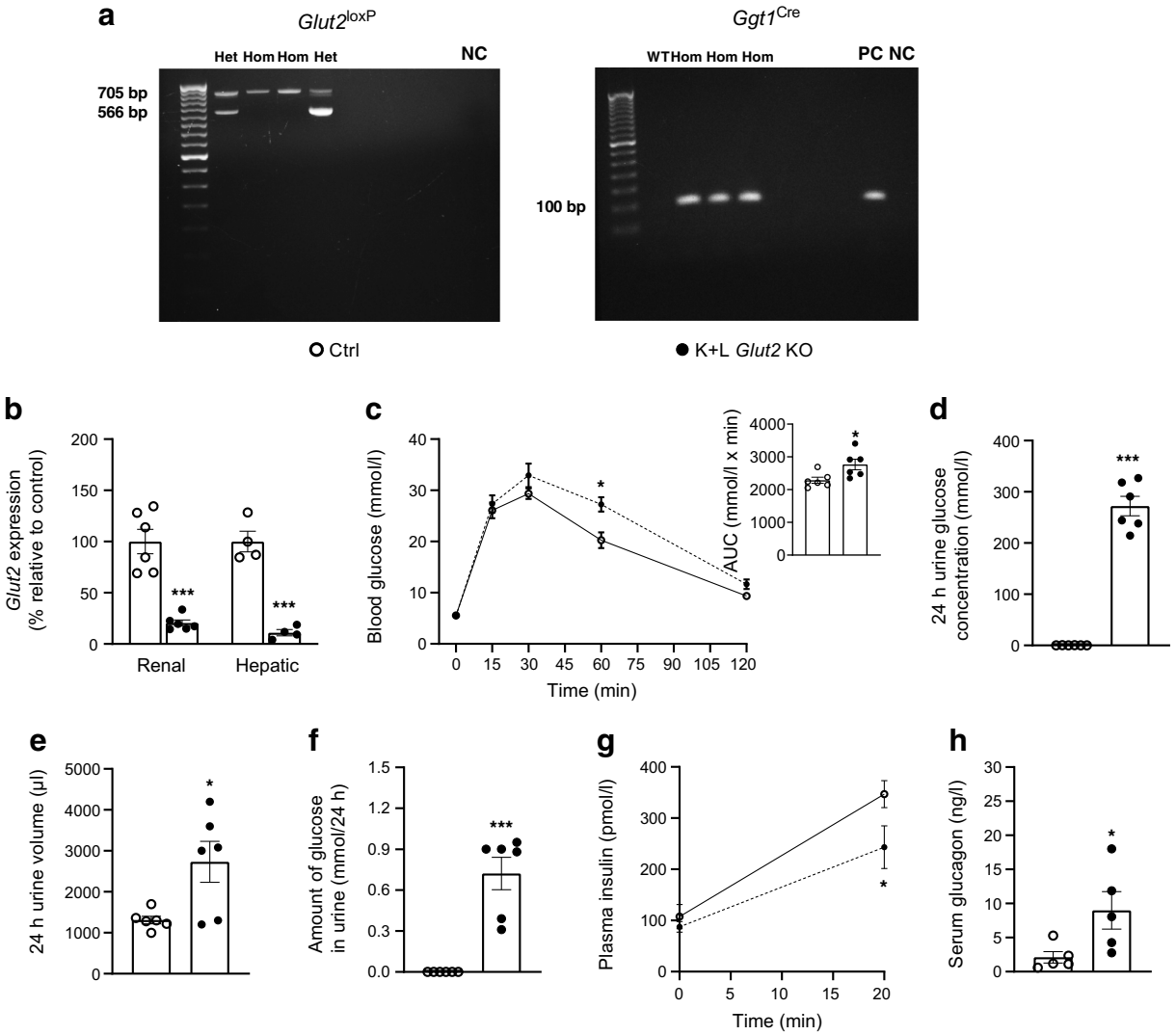

Fig. 3 Mice lacking *Glut2* in the liver in addition to the kidneys show impaired glucose tolerance despite elevated glucosuria. (**a**) Representative genotypes of mice used in this study. *Glut2*^{loxP} mouse model: *Glut2*^{loxP} heterozygous (705 and 566 bp); and *Glut2*^{loxP} homozygous (705 bp). *Ggt1*^{Cre} mouse model: *Ggt1*^{Cre} homozygous (100 bp); and WT (no band). (**b**) Renal cortical and hepatic *Glut2* expression. (**c**) Blood glucose levels during OGTT, with corresponding AUC. (**d**) 24 h urine glucose concentration. (**e**) 24 h urine volume. (**f**) 24 h amount of glucose in urine. (**g**) Plasma insulin levels during oral glucose challenge. (**h**) Serum glucagon levels. Data are shown as means ± SEM for 8- to 12-week-old male mice, n = 4–6. *p<0.05 and ***p<0.001 vs Ctrl group (two-tailed unpaired Student's t test, or one-way ANOVA or repeated measures two-way ANOVA followed by Bonferroni's multiple comparison test). Ctrl, control group; Het, heterozygous; Hom, homozygous; K+L *Glut2* KO, mice with *Glut2* deficiency in the kidneys and liver; NC, negative control; PC, positive control; WT, wild-type

gluconeogenesis (*Pck1* and *G6pc*), only *G6pc* mRNA was elevated in the Ks-*Glut2* KO mice (ESM Fig. 4a,b), indicating that increased gluconeogenesis by *G6pc* was likely to be one of the sources of endogenous glucose that makes up for the loss of glucose in urine. The KO mice had normal GFR, glomerular area and urine pH (ESM Fig. 4c–i), as well as normal kidney weights (both the kidneys combined: control mice, 12 ± 0.2 mg/g body weight; KO mice, 12.8 ± 0.2 mg/g body weight), suggesting the absence of any general renal dysfunction or pathology in these mice.

Mice lacking *Glut2* in the liver in addition to the kidneys do not show improved glucose tolerance despite elevated glucosuria To define and validate the precise contribution of renal GLUT2 to glucose homeostasis relative to the role of other major tissues that also express this glucose transporter, we generated a mouse model that exhibited *Glut2* deficiency in the kidneys and the liver simultaneously by breeding *Ggt1*^{Cre} with the *Glut2*$^{loxP/loxP}$ mice. We had validated the loss of *Glut2* in the liver and renal cortex in *Ggt1*^{Cre};*Glut2*$^{loxP/loxP}$ mice (Fig. 3a,b).

The mice with *Glut2* deficiency in the kidneys and liver (K+L *Glut2* KO) showed impaired glucose tolerance despite massive glucosuria and associated polyuria (male mice, Fig. 3c–f; female mice, ESM Fig. 5a–d). Reduced GSIS (male mice, Fig. 3g; female mice, ESM Fig. 5e) in the K+L *Glut2* KO mice may explain the impairment in their glucose tolerance. Moreover, the K+L *Glut2* KO mice had higher serum glucagon levels (male mice, Fig. 3h; female mice, ESM Fig. 5f), which may have further contributed to their impaired glucose tolerance. These findings reveal the differential physiological contribution of tissue-specific GLUT2 in systemic glucose homeostasis.

Lack of renal *Glut2* reverses hyperglycaemia, improves glucose tolerance and normalises body weight in mouse models of diabetes and obesity In a longitudinal study using mouse models of STZ-induced type 1 diabetes, we observed that Ks-*Glut2* KO mice recovered from STZ-induced hyperglycaemia independently of changes in body weight (Fig. 4a,b) and displayed more severe glucosuria and polyuria (Fig. 4c–e) compared with their control littermates. Notably, the control mice with STZ-induced hyperglycaemia displayed increased renal *Glut2* expression (Fig. 4f) but reduced *Sglt2* mRNA levels (Fig. 4g) compared with the mice that did not receive STZ. These results, which agree with findings from previous studies [19–24, 35], suggest that the reduced renal *Sglt2* could be a compensatory response to suppress glucose reabsorption in diabetes. Despite this decrease in renal *Sglt2*, it was only after induction of renal *Glut2* deficiency that the STZ-induced hyperglycaemia was reversed.

In the HFSD-induced obesity model, we observed that renal *Glut2* deficiency normalised body weight (Fig. 4h), reduced the weight of epididymal fat (Fig. 4i), restored fasting blood glucose and plasma insulin levels, and improved glucose tolerance (Fig. 4j-l) likely via elevated glucosuria (Fig. 4m–o). The renal *Glut2* deficiency did not change food intake (control mice fed HFSD, 2.4 ± 0.02 g/day; Ks-*Glut2* KO mice fed HFSD, 2.3 ± 0.1 g/day), indicating that the reversal of obesity was not due to decreased food consumption. Like STZ, HFSD also increased renal *Glut2* (control diet, 100 ± 15%; HFSD, 141 ± 9% of the control; $p<0.05$) and reduced *Sglt2* (control diet, 100 ± 6%; HFSD, 72 ± 8% of the control; $p<0.05$) mRNA levels, again indicating the importance of inhibiting renal GLUT2 to counteract the enhanced glucose reabsorption caused by diabetes or obesity. At the end of the study, we did verify tamoxifen-induced loss of renal *Glut2* (control mice fed HFSD, 100 ± 14%; Ks-*Glut2* KO mice fed HFSD, 7 ± 1% of the control; $p<0.001$) in HFSD-fed $KspCad^{CreERT2}$;$Glut2^{loxP/loxP}$ mice. Collectively, these findings justify the need for blocking renal GLUT2 for the treatment of diabetes and obesity.

SGLT2 inhibition further improves blood glucose control in Ks-*Glut2* KO mice Dapagliflozin (5 mg/kg, administered by i.p. injection 30 min prior to OGTT) further improved glucose clearance and enhanced glucosuria in the Ks-*Glut2* KO mice (Fig. 5a–d). Based on these promising results, we also evaluated the effects of SGLT2 inhibition on glucose tolerance in Ks-*Glut2* KO mice with either STZ-induced insulin deficiency or HFSD-mediated insulin resistance as described in the longitudinal study mentioned above. Interestingly, dapagliflozin further improved glucose tolerance in these insulin-deficient (Fig. 5e) or insulin-resistant Ks-*Glut2* KO mice (Fig. 5f). Moreover, dapagliflozin (5 mg/kg by i.p. injection at 09:00 and 17:00 hours) increased polyuria, which elevated the total amount of glucose excreted in urine in the Ks-*Glut2* KO mice (Fig. 5g–i). These findings suggest that combined inhibition of SGLT2 and renal GLUT2 may achieve optimal blood glucose control in diabetes.

Long-term renal *Glut2* deficiency almost eliminates *Sglt2* expression via downregulating hepatocyte nuclear factor 1-α To determine the long-term effects of renal *Glut2* deficiency on other renal glucose transporters, we measured their expressions 3 weeks after knocking out renal *Glut2*. Unexpectedly, this long-term renal *Glut2* deficiency dramatically reduced *Sglt2* gene and SGLT2 protein levels (male mice, Fig. 6a–d; female mice, ESM Fig. 6a,b); *Sglt1* was decreased by about 20% without *Glut1* levels being affected (male mice, Fig. 6e,f; female mice, ESM Fig. 6c,d). We had also verified these striking findings using proteomics (ESM Table 1), which showed that there was about 70–80% decrease in renal cortical GLUT2 and SGLT2 as well as no change in GLUT1 and sodium–glucose cotransporter 1 (SGLT1) levels. Therefore, the Ks-*Glut2* KO mice could be utilised as a Ks-*Glut2* and -*Sglt2* double KO mouse model 3 weeks after inducing renal *Glut2* deficiency.

To identify the molecular mechanisms underlying the crosstalk between renal *Glut2* and *Sglt2*, we used a PCR array to screen for renal mouse transcription factors that are downregulated in Ks-*Glut2* KO mice. We observed that a few genes were downregulated by 40–50% (ESM Table 2). Among these genes, *Hnf1α* seemed a likely mediator of the crosstalk between renal GLUT2 and SGLT2 because of its known role in controlling *Sglt2* expression [36–38]. We validated the downregulation of renal *Hnf1α* gene and protein in Ks-*Glut2* KO mice using RT-qPCR, immunohistochemistry and western blotting (male mice, Fig. 6g–i and ESM Fig. 6e; female mice, ESM Fig. 6f). Notably, short-term (within 14 days) renal *Glut2* deficiency did not affect renal *Hnf1α* mRNA levels (control mice, 100 ± 18%; Ks-*Glut2* KO mice, 82 ± 14% of control; $n = 6$). To verify whether recovery of renal *Hnf1α* would restore *Sglt2* and whether re-expression of

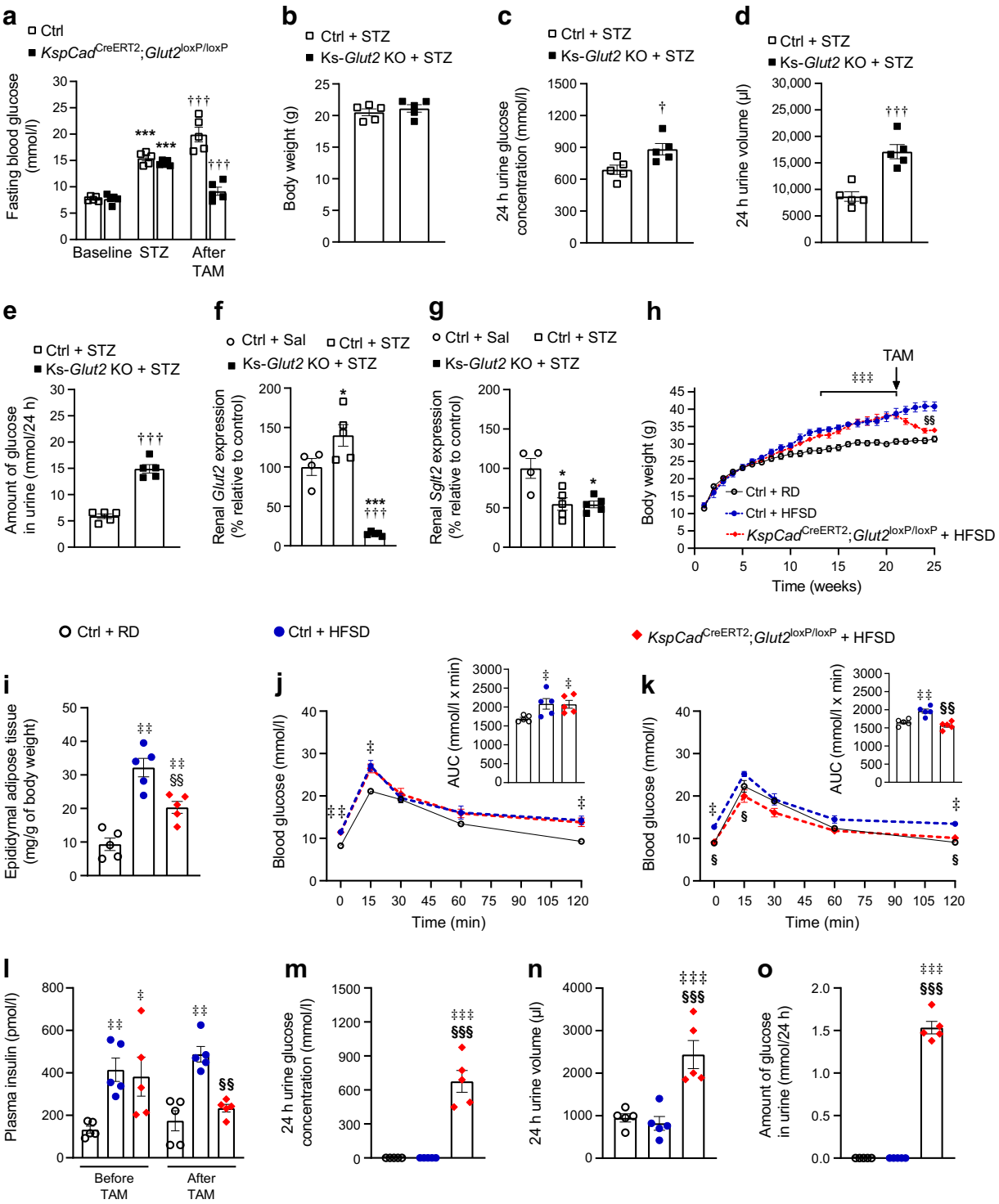

renal *Glut2* would normalise renal *Hnf1α* as well as *Sglt2*, we transfected primary renal proximal tubular epithelial cells isolated from Ks-*Glut2* KO mice (21 days after inducing renal *Glut2* deficiency) with *Hnf1α*- or *Glut2*-expressing plasmids. By the third day of the transfections, *Sglt2* was restored in *Hnf1α*-expressing *Glut2*-deficient cells, and both *Sglt2* and *Hnf1α* were recovered in the cells transfected with *Glut2* (Fig. 6j). These results demonstrate the contribution of renal *Hnf1α* to mediating the crosstalk between renal GLUT2 and SGLT2.

◀ **Fig. 4** Renal *Glut2* deficiency reverses hyperglycaemia and normalises body weight in mouse models of diabetes and obesity. (**a**) Fasting blood glucose levels at baseline, after inducing type 1 diabetes by STZ and on the seventh day after knocking out renal *Glut2* by tamoxifen. (**b**–**e**) Body weight (**b**), 24 h urine glucose concentration (**c**), 24 h urine volume (**d**) and 24 h amount of glucose in urine (**e**) in 8- to 12-week-old female mice with STZ-induced type 1 diabetes before, and on the 12th day after, knocking out renal *Glut2* using tamoxifen. (**f**, **g**) Expression of renal *Glut2* (**f**) and *Sglt2* (**g**) in female mice with STZ-induced type 1 diabetes before, and on the 14th day after, knocking out renal *Glut2*. (**h**) Changes in body weight during 25 weeks of regular diet or HFSD feeding. (**i**) Changes in the weight of epididymal adipose tissue 4 weeks after inducing renal *Glut2* deficiency. (**j**, **k**) Blood glucose levels during OGTT at 1 week pre-renal *Glut2* deficiency (**j**) and on the fifth day post-renal *Glut2* deficiency (**k**). (**l**) Plasma insulin levels 3 days before and on eighth day after renal *Glut2* deficiency. (**m**–**o**) 24 h urine glucose concentration (**m**), 24 h urine volume (**n**) and 24 h amount of glucose in urine (**o**) on the tenth day after inducing renal *Glut2* deficiency in male mice fed a regular diet or HFSD. Data are shown as means ± SEM, $n = 5$. *$p<0.05$ and ***$p<0.001$ vs baseline (**a**) or Ctrl + Sal (**f**, **g**); $^{\dagger}p<0.05$ and $^{\dagger\dagger\dagger}p<0.001$ vs STZ (**a**) or Ctrl + STZ (**c**–**f**); $^{\ddagger}p<0.05$, $^{\ddagger\ddagger}p<0.01$ and $^{\ddagger\ddagger\ddagger}p<0.001$ vs Ctrl + RD; $^{\S}p<0.05$, $^{\S\S}p<0.01$ and $^{\S\S\S}p<0.001$ vs Ctrl + HFSD; (two-tailed unpaired Student's *t* test, or one-way ANOVA or repeated measures two-way ANOVA followed by Bonferroni's multiple comparison test). Ctrl, control $Glut2^{loxP/loxP}$ mice; RD, regular diet; TAM, tamoxifen

Discussion

Here, we have established the physiological contribution of renal GLUT2 to systemic glucose homeostasis using inducible Ks-*Glut2* KO mice. The KO mice exhibited improved glucose tolerance independently of changes in insulin secretion or sensitivity. Moreover, the KO mice recovered from hyperglycaemia in a model of insulin-dependent diabetes within a week after inducing renal *Glut2* deficiency. In a model of diet-induced insulin resistance, renal *Glut2* deficiency normalised glucose tolerance and reversed obesity. We have also identified a novel crosstalk between renal GLUT2 and SGLT2 via the transcription factor HNF1α.

Although GLUT2 is a major glucose transporter in the kidneys, its contribution to systemic glucose homeostasis is not well defined. Previous reports [24, 26], including some from our laboratory [27, 28, 32], have indicated the therapeutic potential of blocking renal GLUT2 in improving blood glucose control through elevated glucosuria. We recently demonstrated that, despite obesity and insulin resistance, hypothalamus-specific *Pomc* and *Mc4r* KO mice exhibit improved glucose tolerance probably because of reduced renal GLUT2 and consequent elevated glucosuria [27, 28, 32]. Based on these findings, we produced Ks-*Glut2* KO mice and assessed their glucose homeostasis in this current study. The KO mice exhibited massive glucosuria and improved glucose tolerance probably because of reduced glucose reabsorption owing to the lack of renal *Glut2*. Moreover, these mice exhibited normal circulating glucagon, NEFA and β-hydroxybutyrate. This phenotype strongly contrasts with that of global *Glut2* KO mice, which show impaired insulin secretion and have elevated plasma levels of glucagon, NEFA and β-hydroxybutyrate [3]. These differences demonstrate the precise contribution of renal GLUT2 to systemic glucose homeostasis, and the lack of effect on other physiological variables that would otherwise have been changed due to global GLUT2 deficiency. Remarkably, the beneficial effects of renal *Glut2* deficiency were abolished when we knocked out *Glut2* in the liver in addition to the kidneys. These results support previous findings that hepatic *Glut2* deficiency impairs glucose homeostasis [39]. Overall, our present study highlights the differential tissue-specific contribution of GLUT2 to systemic glucose homeostasis.

Diabetes increases renal GLUT2 in humans and rodents [19–25], an effect that we have also validated in this present study, thereby enhancing glucose reabsorption and worsening hyperglycaemia. Hence, inhibiting GLUT2 specifically in the kidneys would likely break this vicious cycle and could reverse hyperglycaemia by elevating glucosuria. Indeed, in the present study we observed that inducing *Glut2* deficiency in the kidneys reversed hyperglycaemia in a mouse model of type 1 diabetes and normalised glucose tolerance as well as body weight in a mouse model of diet-induced obesity. These findings provide preclinical evidence that inhibiting renal GLUT2 can reverse diabetes and obesity.

SGLT2 inhibition is an established therapy for treating diabetes [13–18]. However, SGLT2 inhibitors reduce glucose reabsorption by only 30–50%, probably because of the compensation of SGLT1 in the S3 segment, accomplished by GLUT2 or GLUT1 in the basolateral membrane [11, 40–42]. Hence, inhibiting renal GLUT2 may overcome this limitation of SGLT2 inhibitors. *Sglt2* KO mice exhibit massive glucosuria and improved glucose tolerance [12, 18]. In the present study, we show that Ks-*Glut2* KO mice also display a similar degree of glucosuria and improved glucose tolerance, illustrating that renal GLUT2 is as significant as SGLT2 in influencing systemic glucose homeostasis by regulating glucosuria. SGLT2 inhibition increases circulating glucagon, β-hydroxybutyrate and NEFA, causing serious ketoacidosis [43–45]. However, we did not observe these changes or ketoacidosis in Ks-*Glut2* KO mice. These contrasting results indicate that distinct neurohumoral pathways may be involved in either increasing glucose production or utilisation of alternative sources of energy in response to the loss of glucose in urine mediated by blocking the two different glucose transporters. Dapagliflozin further improved glucose tolerance and elevated glucosuria in Ks-*Glut2* KO mice in the presence and absence of diabetes. These findings suggest that combined inhibition of renal GLUT2 and SGLT2 may yield optimal glucose control in diabetes.

Here, we have also identified a previously unknown crosstalk between renal GLUT2 and SGLT2. We have demonstrated that renal *Glut2* deficiency in the long term

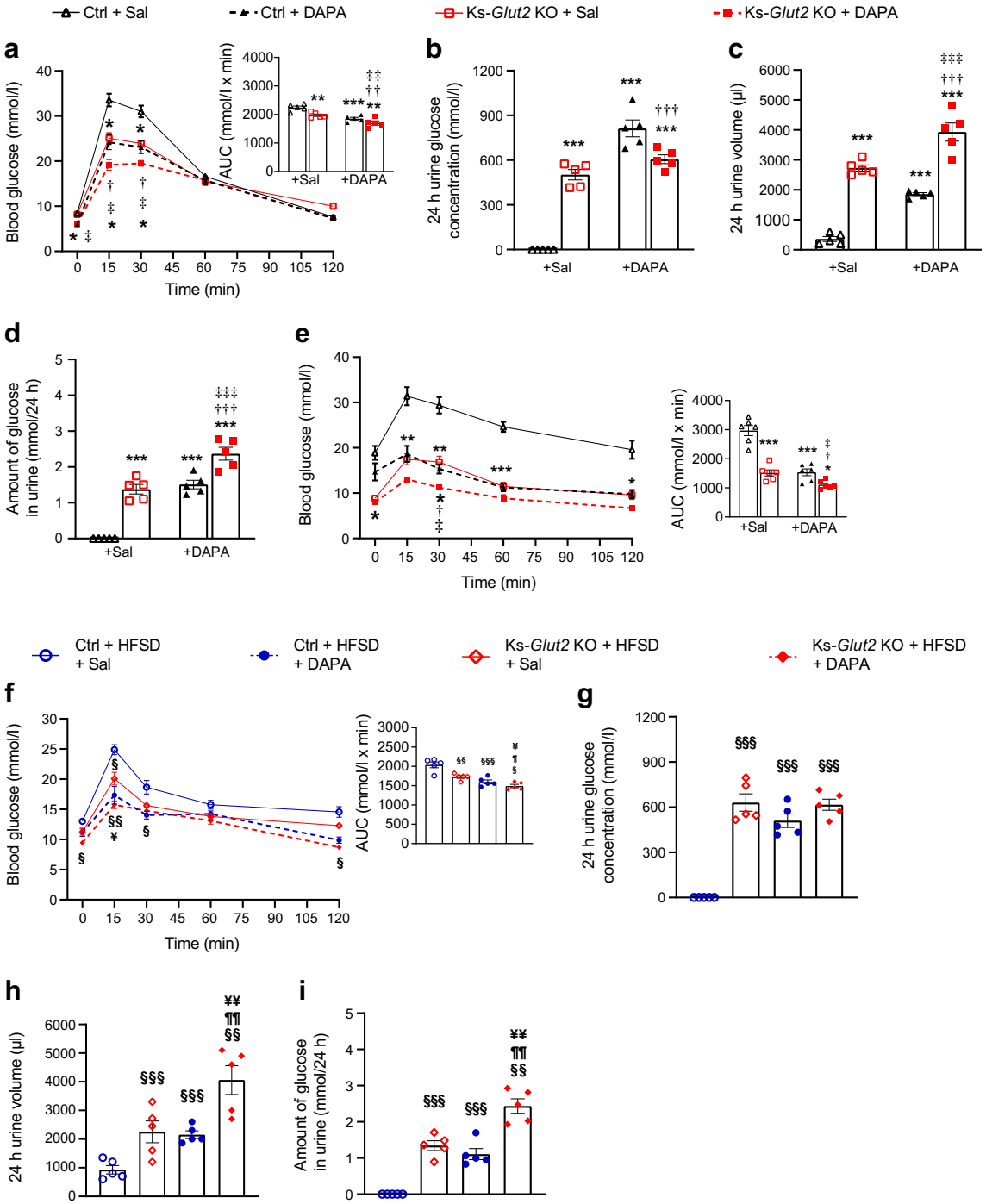

Fig. 5 Dapagliflozin improves glucose tolerance in the absence and presence of diabetes in mice lacking renal *Glut2*. (**a**) Blood glucose levels during OGTT, with corresponding AUC, in 8- to 12-week-old female mice on the seventh day after inducing renal *Glut2* deficiency. (**b**–**d**) 24 h urine glucose concentration (**b**), 24 h urine volume (**c**) and 24 h amount of glucose in urine (**d**) on the 12th day after inducing renal *Glut2* deficiency in 8- to 12-week-old female mice. (**e**) Blood glucose levels during OGTT, with corresponding AUC, on the eighth day after inducing renal *Glut2* deficiency in 8-week-old female mice with STZ-induced type 1 diabetes. (**f**–**i**) Blood glucose levels during OGTT, with corresponding AUC (**f**), 24 h urine glucose concentration (**g**), 24 h urine volume (**h**) and 24 h amount of glucose in urine (**i**) on the 14th day after inducing renal *Glut2* deficiency in HFSD-fed mice. Data are shown as means ± SEM, $n = 5$ or 6. *$p<0.05$, **$p<0.01$ and ***$p<0.001$ vs Ctrl + Sal; $^{\dagger}p<0.05$, $^{\dagger\dagger}p<0.01$ and $^{\dagger\dagger\dagger}p<0.001$ vs Ctrl + DAPA; $^{\ddagger}p<0.05$, $^{\ddagger\ddagger}p<0.01$ and $^{\ddagger\ddagger\ddagger}p<0.001$ vs Ks-*Glut2* KO + Sal; $^{\S}p<0.05$, $^{\S\S}p<0.01$ and $^{\S\S\S}p<0.001$ vs Ctrl + HFSD + Sal; $^{\P}p<0.05$ and $^{\P\P}p<0.01$ vs Ctrl + HFSD + DAPA; $^{¥}p<0.05$ and $^{¥¥}p<0.01$ vs Ks-*Glut2* KO + HFSD +Sal; (repeated measures two-way ANOVA followed by Bonferroni's multiple comparison test). Ctrl, control group; DAPA, dapagliflozin; Sal, saline

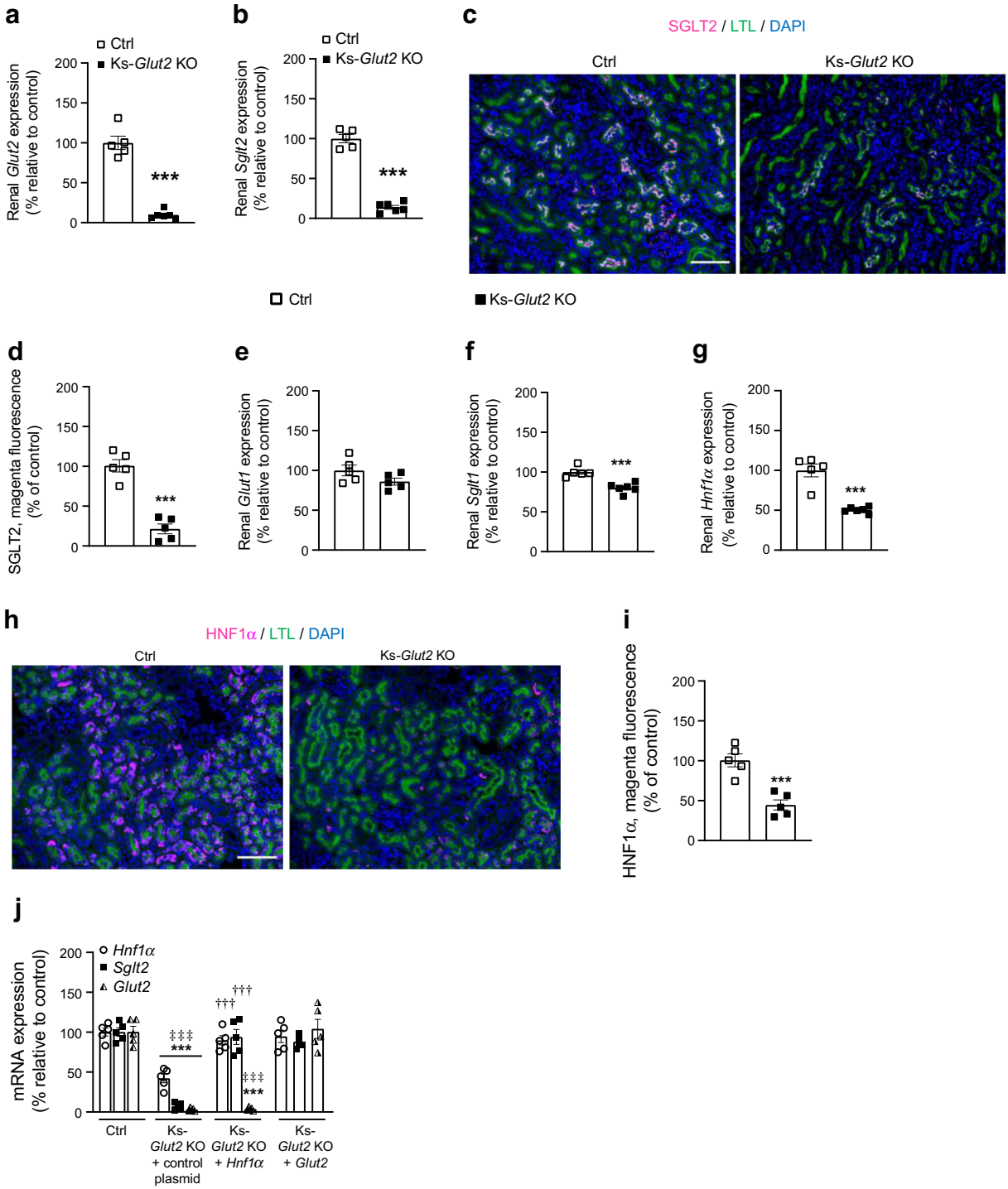

Fig. 6 Long-term renal *Glut2* deficiency almost abolishes the expression of *Sglt2* by downregulating *Hnf1α*. (**a**, **b**) Expression of renal cortical *Glut2* (**a**) and *Sglt2* (**b**). (**c**, **d**) Immunofluorescence staining of renal SGLT2, with its quantification. Scale bar, 100 μm. (**e**–**i**) Expression of renal cortical *Glut1* (**e**), *Sglt1* (**f**) and *Hnf1α* (**g**), and immunofluorescence staining of renal HNF1α as well as its quantification (**h**, **i**), on the 21st day following renal *Glut2* deficiency in 8- to 12-week-old male mice. Scale bar, 100 μm. (**j**) mRNA levels of *Hnf1α, Sglt2* and *Glut2* in primary renal proximal tubular epithelial cells isolated from 8- to 12-week-old male control ($Glut2^{loxP/loxP}$) mice, or mice with kidney-specific loss of *Glut2* (Ks-*Glut2* KO) on the 21st day following renal *Glut2* deficiency. Data are shown as means ± SEM, $n = 5$ or 6. ***$p<0.001$ vs Ctrl; ‡‡‡$p<0.001$ vs Ks-*Glut2* KO + *Glut2*; †††$p<0.001$ vs Ks-*Glut2* KO + control plasmid group (two-tailed unpaired Student's *t* test or two-way ANOVA followed by Bonferroni's multiple comparison test). Ctrl, control $Glut2^{loxP/loxP}$ group; HNF1α, hepatocyte nuclear factor-1α; Ks-*Glut2* KO, *Glut2* knocked out specifically in the kidneys; Ks-*Glut2* KO + *Hnf1α* or *Glut2*, primary renal proximal tubular epithelial cells isolated from Ks-*Glut2* KO mice and transfected with *Hnf1α* or *Glut2* expressing plasmids; LTL, *Lotus tetragonolobus* lectin, a marker of renal proximal tubules

almost abolished the expression of *Sglt2* via downregulating the transcription factor HNF1α. This crosstalk may be clinically significant because *HNF1α* mutations in humans cause elevated glucosuria [36, 46] and monogenic diabetes [46, 47]. Previous studies have demonstrated that *Hnf1α* regulates *Sglt2* expression [36–38]. Therefore, based on these reports and our findings from the current study, elevated glucosuria in individuals with *HNF1α* mutations could be attributed to HNF1α deficiency in the kidneys, and defective insulin secretion could be a result of the lack of HNF1α in beta cells [46]. The crosstalk between *HNF1α* and *SGLT2* may also explain why SGLT2 inhibition produces a higher degree of glucosuria in individuals with *HNF1α* mutations than in those with type 2 diabetes [48]. Collectively, our present study indicates that genetic silencing of renal *Glut2* would also almost eliminate the expression of *Sglt2* by downregulating *Hnf1α*.

This study has some limitations. We did not comprehensively investigate why K+L *Glut2* KO mice display impaired glucose tolerance despite elevated glucosuria. We did report that increased glucagon and defective GSIS in these mice could have contributed to their impaired glucose tolerance, although other developmental factors arising from hepatic *Glut2* deficiency since birth may also have negatively affected glucose homeostasis in these mice. While we have demonstrated in the present study that loss of function of renal *Glut2* in the long-term almost abolishes *Sglt2* expression via downregulation of renal *Hnf1α*, it remains unclear whether the reverse is true (i.e. whether genetic *Sglt2* deficiency would eliminate the expression of *Glut2*). *Sglt2* null mice have normal renal *Glut2* expression at a specific age [12] but this outcome may change over time based on our observation in the present study that renal *Glut2* deficiency causes a progressive decrease in renal *Sglt2* expression. Although we had observed that renal *Glut2* deficiency reversed diet-induced obesity, precise mechanisms underlying this phenotype remain unclear. The loss of energy through elevated glucosuria is one contributing factor to reversing the obesity but other mechanisms [49–51] such as enhanced lipolysis, increased energy expenditure and/or reduced inflammation in normalising body weight in Ks-*Glut2* KO mice need further investigation.

Altogether, findings from this study demonstrate that inhibiting renal GLUT2 can reverse hyperglycaemia and obesity in mice. Moreover, combined inhibition of renal GLUT2 and SGLT2 may achieve optimal blood glucose control in diabetes. We have also uncovered a novel crosstalk between renal GLUT2 and SGLT2 via the transcription factor HNF1α, which raises the possibility that some of the clinical features of Fanconi–Bickel syndrome may be secondary to the downregulation of *HNF1α* and *SGLT2*.

Supplementary Information The online version contains peer-reviewed but unedited supplementary material available at https://doi.org/10.1007/s00125-022-05676-8.

Acknowledgements We thank the following people: J. LaFontaine, University of Alabama at Birmingham, for help with GFR measurements; G. Pryhuber, C. Poole and S. Mack, University of Rochester Medical Center Paediatric Histology Service (URMC-PHS), for help with histology; V. K. Thomas and J. Zhang, URMC Center for Advanced Light Microscopy and Nanoscopy, for help with microscopy; and K. Welle, University of Rochester Mass Spectrometry Resource Laboratory, for proteomics and [$^{13}C_6$]glucose assay.

Data availability All data are available in the main text or the supplementary materials. Additional raw data are available upon request to the corresponding author. The mouse models used in this study are available via material transfer agreement addressed to the corresponding author.

Funding Funding sources are as follows: National Institutes of Health grant DK124619 (KHC); National Institutes of Health grant DK122190 (KHC); National Institutes of Health grant DK113115 (KHC); Startup funds and pilot research award, Department of Medicine, University of Rochester, NY (KHC); National Institutes of Health grant DK079337 (UAB-UCSD O'Brien Core Center for Acute Kidney Injury Research); The Department of Paediatrics, University of Rochester, NY (URMC-PHS); National Institutes of Health grant HL148861(URMC-PHS); Pilot and feasibility award funded by the Pennington Biomedical NORC DK072476 (DHM). American Diabetes Association Junior Faculty Award 1-15-JF-37 (DHM); and National Institutes of Health instrument grant OD025242 to University of Rochester Mass Spectrometry Resource Laboratory.

Authors' relationships and activities The authors declare that there are no relationships or activities that might bias, or be perceived to bias, their work.

Contribution statement LMdSC and LB designed and performed experiments, analysed results, prepared graphs and figures, and edited the manuscript. ND genotyped the mice, performed experiments, and edited the manuscript. DHM provided *Glut2*$^{loxP/loxP}$ mice and edited the manuscript. DJMP provided *KspCad*^{CreERT2} mice and edited the manuscript. KHC conceived the study, designed and performed experiments, analysed results, prepared graphs and figures, and wrote and edited the manuscript. All the authors approved the final version of the manuscript. KHC is the guarantor of this work.

References

1. Thorens B, Cheng ZQ, Brown D, Lodish HF (1990) Liver glucose transporter: a basolateral protein in hepatocytes and intestine and kidney cells. Am J Phys 259(6 Pt 1):C279–C285. https://doi.org/10.1152/ajpcell.1990.259.2.C279
2. Thorens B, Sarkar HK, Kaback HR, Lodish HF (1988) Cloning and functional expression in bacteria of a novel glucose transporter present in liver, intestine, kidney, and β-pancreatic islet cells. Cell 55(2):281–290. https://doi.org/10.1016/0092-8674(88)90051-7
3. Guillam MT, Hümmler E, Schaerer E et al (1997) Early diabetes and abnormal postnatal pancreatic islet development in mice lacking Glut-2. Nat Genet 17(3):327–330. https://doi.org/10.1038/ng1197-327
4. De Vos A, Heimberg H, Quartier E et al (1995) Human and rat beta cells differ in glucose transporter but not in glucokinase gene expression. J Clin Invest 96(5):2489–2495. https://doi.org/10.1172/jci118308
5. McCulloch LJ, van de Bunt M, Braun M, Frayn KN, Clark A, Gloyn AL (2011) GLUT2 (SLC2A2) is not the principal glucose

transporter in human pancreatic beta cells: implications for understanding genetic association signals at this locus. Mol Genet Metab 104(4):648–653. https://doi.org/10.1016/j.ymgme.2011.08.026
6. Santer R, Schneppenheim R, Suter D, Schaub J, Steinmann B (1998) Fanconi-Bickel syndrome–the original patient and his natural history, historical steps leading to the primary defect, and a review of the literature. Eur J Pediatr 157(10):783–797. https://doi.org/10.1007/s004310050937
7. Santer R, Schneppenheim R, Dombrowski A, Götze H, Steinmann B, Schaub J (1997) Mutations in GLUT2, the gene for the liver-type glucose transporter, in patients with Fanconi-Bickel syndrome. Nat Genet 17(3):324–326. https://doi.org/10.1038/ng1197-324
8. Sansbury FH, Flanagan SE, Houghton JA et al (2012) SLC2A2 mutations can cause neonatal diabetes, suggesting GLUT2 may have a role in human insulin secretion. Diabetologia 55(9):2381–2385. https://doi.org/10.1007/s00125-012-2595-0
9. Khandelwal P, Sinha A, Jain V, Houghton J, Hari P, Bagga A (2018) Fanconi syndrome and neonatal diabetes: phenotypic heterogeneity in patients with GLUT2 defects. CEN Case Rep 7(1):1–4. https://doi.org/10.1007/s13730-017-0278-x
10. Beermann F, Thorens B, Guillam M-T, Burcelin R, Jaquet M (2000) Transgenic Reexpression of GLUT1 or GLUT2 in pancreatic β cells rescues GLUT2-null mice from early death and restores normal glucose-stimulated insulin secretion. J Biol Chem 275(31):23751–23758. https://doi.org/10.1074/jbc.M002908200
11. Ghezzi C, Loo DDF, Wright EM (2018) Physiology of renal glucose handling via SGLT1, SGLT2 and GLUT2. Diabetologia 61(10):2087–2097. https://doi.org/10.1007/s00125-018-4656-5
12. Vallon V, Platt KA, Cunard R et al (2011) SGLT2 mediates glucose reabsorption in the early proximal tubule. J Am Soc Nephrol 22(1):104–112. https://doi.org/10.1681/asn.2010030246
13. Abdul-Ghani MA, DeFronzo RA (2008) Inhibition of renal glucose reabsorption: a novel strategy for achieving glucose control in type 2 diabetes mellitus. Endocr Pract 14(6):782–790. https://doi.org/10.4158/ep.14.6.782
14. DeFronzo RA, Hompesch M, Kasichayanula S et al (2013) Characterization of renal glucose reabsorption in response to dapagliflozin in healthy subjects and subjects with type 2 diabetes. Diabetes Care 36(10):3169–3176. https://doi.org/10.2337/dc13-0387
15. Santer R, Kinner M, Lassen CL et al (2003) Molecular analysis of the SGLT2 gene in patients with renal Glucosuria. J Am Soc Nephrol 14(11):2873–2882. https://doi.org/10.1097/01.Asn.0000092790.89332.D2
16. Rossetti L, Smith D, Shulman GI, Papachristou D, DeFronzo RA (1987) Correction of hyperglycemia with phlorizin normalizes tissue sensitivity to insulin in diabetic rats. J Clin Invest 79(5):1510–1515. https://doi.org/10.1172/JCI112981
17. Oku A, Ueta K, Arakawa K et al (1999) T-1095, an inhibitor of renal Na+−glucose cotransporters, may provide a novel approach to treating diabetes. Diabetes 48(9):1794–1800. https://doi.org/10.2337/diabetes.48.9.1794
18. Vallon V, Rose M, Gerasimova M et al (2013) Knockout of Na-glucose transporter SGLT2 attenuates hyperglycemia and glomerular hyperfiltration but not kidney growth or injury in diabetes mellitus. Am J Physiol Renal Physiol 304(2):F156–F167. https://doi.org/10.1152/ajprenal.00409.2012
19. Rahmoune H, Thompson PW, Ward JM, Smith CD, Hong G, Brown J (2005) Glucose transporters in human renal proximal tubular cells isolated from the urine of patients with non–insulin-dependent diabetes. Diabetes 54(12):3427–3434. https://doi.org/10.2337/diabetes.54.12.3427
20. Dominguez JH, Camp K, Maianu L, Feister H, Garvey WT (1994) Molecular adaptations of GLUT1 and GLUT2 in renal proximal tubules of diabetic rats. Am J Phys 266(2 Pt 2):F283–F290. https://doi.org/10.1152/ajprenal.1994.266.2.F283
21. Marks J, Carvou NJ, Debnam ES, Srai SK, Unwin RJ (2003) Diabetes increases facilitative glucose uptake and GLUT2 expression at the rat proximal tubule brush border membrane. J Physiol 553(Pt 1):137–145. https://doi.org/10.1113/jphysiol.2003.046268
22. Kamran M, Peterson RG, Dominguez JH (1997) Overexpression of GLUT2 gene in renal proximal tubules of diabetic Zucker rats. J Am Soc Nephrol 8(6):943–948. https://doi.org/10.1681/ASN.V86943
23. Chin E, Zamah AM, Landau D et al (1997) Changes in facilitative glucose transporter messenger ribonucleic acid levels in the diabetic rat kidney. Endocrinology 138(3):1267–1275. https://doi.org/10.1210/endo.138.3.5015
24. Hinden L, Udi S, Drori A et al (2018) Modulation of renal GLUT2 by the Cannabinoid-1 receptor: implications for the treatment of diabetic nephropathy. J Am Soc Nephrol 29(2):434–448. https://doi.org/10.1681/ASN.2017040371
25. Jiang Y-K, Xin K-Y, Ge H-W, Kong F-J, Zhao G (2019) Upregulation of renal GLUT2 and SGLT2 is involved in high-fat diet-induced gestational diabetes in mice. Diabetes Metab Syndr Obes 12:2095–2105. https://doi.org/10.2147/DMSO.S221396
26. Liu X-J, Wu X-Y, Wang H et al (2018) Renal injury in Seipin-deficient lipodystrophic mice and its reversal by adipose tissue transplantation or leptin administration alone: adipose tissue-kidney crosstalk. FASEB J 32(10):5550–5562. https://doi.org/10.1096/fj.201701427R
27. Chhabra KH, Adams JM, Fagel B et al (2016) Hypothalamic POMC deficiency improves glucose tolerance despite insulin resistance by increasing glycosuria. Diabetes 65(3):660–672. https://doi.org/10.2337/db15-0804
28. de Souza Cordeiro LM, Elsheikh A, Devisetty N et al (2021) Hypothalamic MC4R regulates glucose homeostasis through adrenaline-mediated control of glucose reabsorption via renal GLUT2 in mice. Diabetologia 64(1):181–194. https://doi.org/10.1007/s00125-020-05289-z
29. Lantinga-van Leeuwen IS, Leonhard WN, van de Wal A et al (2006) Transgenic mice expressing tamoxifen-inducible Cre for somatic gene modification in renal epithelial cells. Genesis 44(5):225–232. https://doi.org/10.1002/dvg.20207
30. Lantinga-van Leeuwen IS, Leonhard WN, van der Wal A, Breuning MH, de Heer E, Peters DJ (2007) Kidney-specific inactivation of the Pkd1 gene induces rapid cyst formation in developing kidneys and a slow onset of disease in adult mice. Hum Mol Genet 16(24):3188–3196. https://doi.org/10.1093/hmg/ddm299
31. Leonhard WN, Happe H, Peters DJM (2016) Variable cyst development in autosomal dominant polycystic kidney disease: the biologic context. J Am Soc Nephrol 27(12):3530–3538. https://doi.org/10.1681/asn.2016040425
32. Chhabra KH, Morgan DA, Tooke BP, Adams JM, Rahmouni K, Low MJ (2017) Reduced renal sympathetic nerve activity contributes to elevated glycosuria and improved glucose tolerance in hypothalamus-specific Pomc knockout mice. Mol Metab 6(10):1274–1285. https://doi.org/10.1016/j.molmet.2017.07.005
33. Ding W, Yousefi K, Shehadeh LA (2018) Isolation, characterization, and high throughput extracellular flux analysis of mouse primary renal tubular epithelial cells. J Vis Exp 136:57718. https://doi.org/10.3791/57718
34. Schreiber A, Shulhevich Y, Geraci S et al (2012) Transcutaneous measurement of renal function in conscious mice. Am J Physiol Renal Physiol 303(5):F783–F788. https://doi.org/10.1152/ajprenal.00279.2012
35. Albertoni Borghese MF, Majowicz MP, Ortiz MC, Passalacqua Mdel R, Sterin Speziale NB, Vidal NA (2009) Expression and activity of SGLT2 in diabetes induced by streptozotocin: relationship with the lipid environment. Nephron Physiol 112(3):p45–p52. https://doi.org/10.1159/000214214

36. Pontoglio M, Prié D, Cheret C et al (2000) HNF1alpha controls renal glucose reabsorption in mouse and man. EMBO Rep 1(4): 359–365. https://doi.org/10.1093/embo-reports/kvd071
37. Freitas HS, Schaan BD, David-Silva A et al (2009) SLC2A2 gene expression in kidney of diabetic rats is regulated by HNF-1alpha and HNF-3beta. Mol Cell Endocrinol 305(1–2):63–70. https://doi.org/10.1016/j.mce.2009.02.014
38. Umino H, Hasegawa K, Minakuchi H et al (2018) High basolateral glucose increases sodium-glucose cotransporter 2 and reduces Sirtuin-1 in renal tubules through glucose Transporter-2 detection. Sci Rep 8(1):6791. https://doi.org/10.1038/s41598-018-25054-y
39. Seyer P, Vallois D, Poitry-Yamate C et al (2013) Hepatic glucose sensing is required to preserve β cell glucose competence. J Clin Invest 123(4):1662–1676. https://doi.org/10.1172/JCI65538
40. Powell DR, DaCosta CM, Gay J et al (2013) Improved glycemic control in mice lacking Sglt1 and Sglt2. Am J Physiol Endocrinol Metab 304(2):E117–E130. https://doi.org/10.1152/ajpendo.00439.2012
41. Chin E, Zhou J, Bondy C (1993) Anatomical and developmental patterns of facilitative glucose transporter gene expression in the rat kidney. J Clin Invest 91(4):1810–1815. https://doi.org/10.1172/jci116392
42. Liu JJ, Lee T, DeFronzo RA (2012) Why do SGLT2 inhibitors inhibit only 30-50% of renal glucose reabsorption in humans? Diabetes 61(9):2199–2204. https://doi.org/10.2337/db12-0052
43. Perry RJ, Rabin-Court A, Song JD et al (2019) Dehydration and insulinopenia are necessary and sufficient for euglycemic ketoacidosis in SGLT2 inhibitor-treated rats. Nat Commun 10(1):548–548. https://doi.org/10.1038/s41467-019-08466-w
44. Peters AL, Buschur EO, Buse JB, Cohan P, Diner JC, Hirsch IB (2015) Euglycemic diabetic ketoacidosis: a potential complication of treatment with sodium–glucose cotransporter 2 inhibition. Diabetes Care 38(9):1687–1693. https://doi.org/10.2337/dc15-0843
45. Erondu N, Desai M, Ways K, Meininger G (2015) Diabetic ketoacidosis and related events in the Canagliflozin type 2 diabetes clinical program. Diabetes Care 38(9):1680–1686. https://doi.org/10.2337/dc15-1251
46. Pontoglio M, Sreenan S, Roe M et al (1998) Defective insulin secretion in hepatocyte nuclear factor 1alpha-deficient mice. J Clin Invest 101(10):2215–2222. https://doi.org/10.1172/jci2548
47. Yamagata K, Oda N, Kaisaki PJ et al (1996) Mutations in the hepatocyte nuclear factor-1alpha gene in maturity-onset diabetes of the young (MODY3). Nature 384(6608):455–458. https://doi.org/10.1038/384455a0
48. Hohendorff J, Szopa M, Skupien J et al (2017) A single dose of dapagliflozin, an SGLT-2 inhibitor, induces higher glycosuria in GCK- and HNF1A-MODY than in type 2 diabetes mellitus. Endocrine 57(2):272–279. https://doi.org/10.1007/s12020-017-1341-2
49. Xu L, Nagata N, Nagashimada M et al (2017) SGLT2 inhibition by Empagliflozin promotes fat utilization and Browning and Attenuates inflammation and insulin resistance by polarizing M2 macrophages in diet-induced obese mice. EBioMedicine 20:137–149. https://doi.org/10.1016/j.ebiom.2017.05.028
50. Osataphan S, Macchi C, Singhal G et al (2019) SGLT2 inhibition reprograms systemic metabolism via FGF21-dependent and -independent mechanisms. JCI Insight 4(5). https://doi.org/10.1172/jci.insight.123130
51. Yokono M, Takasu T, Hayashizaki Y et al (2014) SGLT2 selective inhibitor ipragliflozin reduces body fat mass by increasing fatty acid oxidation in high-fat diet-induced obese rats. Eur J Pharmacol 727: 66–74. https://doi.org/10.1016/j.ejphar.2014.01.040